

# A Reduced-order Time-Frequency Transforming Method for Non-Stationary Vibration Analysis

Javad Isavand<sup>a</sup>, Andrew Peplow<sup>b</sup>, Jihong Yan<sup>a\*</sup>

<sup>a</sup> School of Mechatronics Engineering, Harbin Institute of Technology, Harbin, China.

<sup>b</sup> Principal Acoustic Consultant, Hawkins & Associates, Cambridge, England.

\* Corresponding author e-mail: [jyan@hit.edu.cn](mailto:jyan@hit.edu.cn)

## Abstract

This paper introduces a novel time-frequency signal analysis method for analysing non-stationary signals called the Reduced-order Time-Frequency Transform (RTFT). Spectral analysis using the Fourier Transform is effective for stationary time series where signal characteristics remain constant over time. However, for non-stationary time series such as modulated signals, the spectral content varies with time, thus rendering the time-averaged amplitude spectrum derived from the Fourier Transform insufficient for tracking changes in signal magnitude, frequency, or phase. The RTFT technique offers the capabilities of traditional time-frequency transformations by employing Pearson's Correlation Coefficient to selectively reduce the data volume in the joint time-frequency domain. This method emphasizes highly correlated frequencies and phases leading to a more efficient data representation without significant loss of accuracy. The RTFT is validated through comparative analysis with established methods, including the Short-Time Fourier Transform (STFT), Hilbert-Huang Transform (HHT), Fourier Synchrosqueezed Transform (FSST), and Wavelet Synchrosqueezed Transform (WSST). A non-stationary synthesized and real-world vibration-based condition monitoring signal is analysed using both RTFT and the traditional methods to demonstrate the superiority of the RTFT in reducing data volume while maintaining accuracy.

**Keywords:** Time-Frequency Analysis; Condition Monitoring; Data Volume Reduction.

---

## 1. Introduction

Non-stationary time series inherently change over time, meaning their statistical characteristics evolve or change with time. Processing these series as a single entity in the time or frequency domain consistently fails to capture important information which is essentially a consequence of the statistical characteristics changing with time[1]. Consequently, extensive research has been devoted to developing a diverse range of time-frequency methods for more accurate and reliable analysis.

However, to date no single method has yet been developed that can comprehensively address all non-time-invariant transforms. So, in this introduction we shall review several key methods recognized within the research and scientific community of which four stand-out. These include Time-Frequency Distributions (TFD), Wavelet Transforms (WT), data-driven decomposition methods and finally Synchrosqueezed approaches. The reader can read more details about these and other methods within the 2021 review by Akan and Cura, [2].

Nonetheless, Time-Frequency Distribution (TFD) methods can basically be categorized into linear and nonlinear techniques. The Short-Time Fourier Transform (STFT), a linear technique, segmenting the time series using a sliding window and computes the Fourier transform of each segment, [3]. This was a common technique for a few decades but in 1995, Cohen introduced a nonlinear TFD method known as Cohen's class of Bilinear Distribution (BD), which computes the Fourier transform of a time-varying covariance function using a kernel function, [4]. Various BD techniques, such as the Wigner-Ville Distribution, Choi-Williams Kernel, and Cone Kernel, have been developed to achieve high-resolution energy distribution [2,5]. Similarly, the Gabor Transform applies a sliding Gaussian function to transform time series into the time-frequency domain, while the Stockwell Transform (S-transform) enhances the Gabor Transform by using a frequency-dependent Gaussian window, resulting in better performance, [5,6].

In contrast to the STFT's uniform window, the Wavelet Transform (WT) uses a diverse range of filters with varying bandwidths across frequencies. Research on continuous and discrete wavelet transforms has enhanced accuracy by utilizing various mother wavelet forms, such as Haar, Daubechies, Coiflet, Morlet, Meyer, and the Mexican Hat [7–9]. For example, the Malvar expansion presents a wavelet-based approach with windowing techniques determined by an entropy measure, representing signals with discrete cosine functions, [10].

Data-driven decomposition methods have gained significant attention in recent times, aiming to decompose signals into zero-mean Intrinsic Mode Functions (IMFs). The Hilbert-Huang Transform (HHT) applied to Empirical Mode Decomposition (EMD) and its derivatives, such as Bivariate Empirical Mode Decomposition (BEMD), Multivariate Empirical Mode Decomposition (MEMD), and Ensemble Empirical Mode Decomposition (EEMD), are widely used [11–14]. Other methods include Variational Mode Decomposition (VMD), Fourier Mode Decomposition (FMD), and Dynamic Mode Decomposition (DMD), [15–17].

And finally, Synchrosqueezed Transform techniques (SST) and Reassignment Methods (RM) which have been explored to enhance time and frequency accuracy. The Fourier Synchrosqueezing Transform (FSST) refines the STFT by estimating instantaneous frequency and selecting corresponding STFT coefficients [18,19]. The Wavelet Synchrosqueezing Transform (WSST) incorporates instantaneous frequency into wavelet methods, achieving higher accuracy and robustness [9].

Despite improvements in accuracy, various transforming techniques described above face challenges such as mode mixing, cross-term errors, and high-frequency harmonic distortion, [20,21]. Recently, a machine-learning-based method for fault recognition in tool condition monitoring proposed a novel joint time-frequency transforming technique, producing clearer time-frequency spectrums but with high computational costs [24]. To address these challenges, a reduced-order machine-learning-based method has been recently proposed for fault recognition in tool condition monitoring using machine learning (ML) techniques. This ML-based method introduces an innovative joint time-frequency transforming technique. Although this approach results in clearer time-frequency spectrums, making failure symptom recognition more straightforward and reducing data volume compared to other methodologies, it still incurs high computational costs due to the numerous fitting processes. Hence, this study presents a novel reduced-order time-frequency transform technique to address these challenges.

## 2. Methodology

The reduced-order time frequency method divides a non-stationary time series into several short-time segments and considers each segment as a summation of stationary functions. This section presents the fundamental concept and formulation of the proposed RTFT method. The method can be expressed, mathematically as follows:

$$X_j(t) = \sum_i c_{ij}(t) h_{ij}(t) \quad (1)$$

where  $X_j(t)$  represents the  $j^{\text{th}}$  segment in the given signal,  $c_{ij}(t)$  denotes the coefficients, and  $h_{ij}(t)$  corresponds the basis functions. In accordance with the Gabor expansion, if the time segments are selected short enough, the coefficients,  $c_{ij}(t)$ , can be approximately assumed as constant values which results in  $X_j(t) \approx \sum c_{ij} h_{ij}(t)$ , [2]. Then, by assuming  $h_{ij}(t)$  as summation of basis functions,  $\sum_i \sin(2\pi\omega_{ij}t + \varphi_{ij})$ , it is possible to estimate the original signal among the  $j^{\text{th}}$  short-time segment calculating unknown parameters such as frequencies and phases. It should be noted that the basis functions can be chosen as either sine or cosine functions:

$$\hat{X}_j(t) = \sum_{i=1}^{\mathcal{M}_j} \sin(2\pi\omega_{ij}t + \varphi_{ij}) \quad (2)$$

where the estimated time series for the  $j^{\text{th}}$  segment is represented by  $\hat{X}_j(t)$ . The model order, frequency in Hertz, and phase difference in the  $j^{\text{th}}$  short-time segment are denoted as  $\mathcal{M}_j$ ,  $\omega_{ij}$ , and  $\varphi_{ij}$ , respectively. As shown in Fig.1, a schematic diagram is presented to clarify the algorithm of the methodology. The RTFT technique divides a non-stationary signal into several short-time segments using a fixed rectangular window over time. Then, the Pearson's correlation coefficient is calculated separately between each segment of the original time series and the basis function, including all individual frequencies ranging from 0 to  $F_{max}$ .

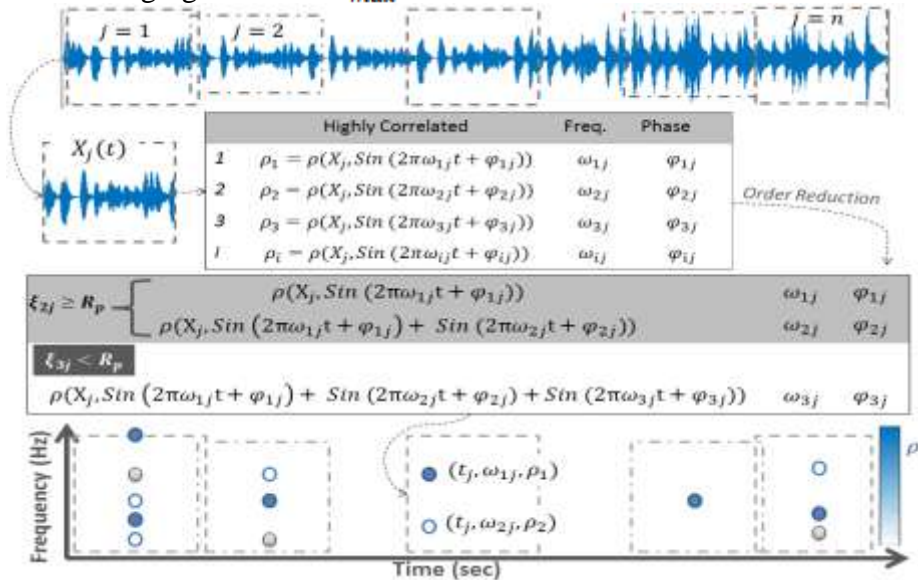


**Figure 1.** The structure of the Reduced-order Time-Frequency Transform (RTFT) method

The calculated correlation coefficients are then sorted, enabling the identification and ranking of the most influential frequencies, starting from the highest correlated frequency. Via the summation in Eq. (2), the expression in Eq. (3) represents the assumed summation and Pearson's correlation function:

$$\rho(X_j, \hat{X}_j) = \frac{1}{N_{max} - 1} \sum_{i=1}^{N_{max}} \left( \frac{x_{ij} - \mu_{X_j}}{\sigma_{X_j}} \right) \left( \frac{\hat{x}_{ij} - \mu_{\hat{X}_j}}{\sigma_{\hat{X}_j}} \right) = \frac{\langle X_j^{Norm}, \hat{X}_j^{Norm} \rangle}{N_{max} - 1} \quad (3)$$

According to the definition of the Pearson's correlation coefficient, the signals become normalized with zero-mean and unit-variance, shown by superscript '*Norm*'. Where  $\sigma$  and  $\mu$  are the standard deviation and mean of the time series, while  $N_{max}$  signifies the number of data in each segment. It is noted that the phase difference can play a significant role in influencing the Pearson's correlation coefficient. Thus, determining this parameter is crucial to achieving the highest correlation. While the optimal frequencies and phases,  $\max_{\omega_{ij}, \varphi_{ij}} |\rho(X_j, \hat{X}_j)|$ , can be calculated iteratively, this approach leads to an increase in runtime complexity to  $O(n^2)$ . To optimize this process and reduce runtime, the optimal frequencies can be calculated iteratively while the optimal phases are derived mathematically using the following expressions. However, the runtime complexity exhibits a loglinear relationship with the frequency range and resolution. Similar to other well-established methods, the runtime complexity can be considered as  $O(n \log n)$ ,

$$\max_{\varphi_{ij}} |\langle X_j^{Norm}, \hat{X}_{ij} \rangle| = \max_{\varphi_{ij}} |\langle X_j^{Norm}, \sin(2\pi\omega_{ij}t + \varphi_{ij}) \rangle| \quad (4)$$

where optimal frequencies can be calculated iteratively, and the optimal phases determined below by calculating the derivative of Eq. (4) with respect to  $\varphi_{ij}$ :

$$\varphi_{ij} = \tan^{-1} \left( \frac{\langle X_j^{Norm}, \cos(2\pi\omega_{ij}t) \rangle}{\langle X_j^{Norm}, \sin(2\pi\omega_{ij}t) \rangle} \right) \quad (5)$$

In this case, the correlation between the signal and cosine functions,  $\langle X_j^{Norm}, \cos(2\pi\omega_{ij}t) \rangle$ , can conceptually be considered similar to the Discrete Cosine Transform (DCT), [24]. In contrast with the well-known discrete cosine transform, DCT, for the RTFT method the frequency resolution does not depend on the amount of data in each segment.

To determine the model order,  $\mathcal{M}_j$ , various factors need to be reviewed. It is generally accepted that if the amplitudes are considered, increasing the model order generally leads to higher correlation coefficients and improved estimation accuracy. However, this comes at a cost of increased computational load. In this case by neglecting the amplitudes and only considering frequencies and phases, it is possible to reduce computational costs, although it makes the methodology most challenging for signal reconstruction. Therefore, it is crucial to find an optimal balance between accuracy and computational efficiency. To address this, a correlation change level can be utilized to select the optimal model order. This involves calculating the correlation changes between different model orders, and aiming for a desired correlation change between the original signal and the basis model within the selected period. As frequencies and phases are ranked based on the highest calculated correlations, they are progressively added to the summation if the new correlation coefficient exceeds the previous coefficient multiplied by a predefined participation ratio called the ratio of participation,  $R_p$ :

$$\xi_{mj} = \begin{cases} \frac{\rho(X_j, \hat{X}_j^m)}{\rho(X_j, \hat{X}_j^{m-1})} = \frac{\rho(X_j, \sum_{i=1}^m \sin(2\pi\omega_{ij}t + \varphi_{ij}))}{\rho(X_j, \sum_{i=1}^{m-1} \sin(2\pi\omega_{ij}t + \varphi_{ij}))} & m \geq 2 \\ R_p & m = 1 \end{cases} \quad (6)$$

where  $\omega_{ij}$  and  $\varphi_{ij}$  represent the frequency and phase related to the  $i^{th}$  highest correlation coefficient within the  $j^{th}$  segment. In essence, the impact of the ratio  $\xi_{mj}$  can be explained as follows: the method sorts the frequencies according to their highest correlations and treats the first-ranked frequency as the initial estimate. Subsequently, additional frequencies are incorporated into the sine summation of the estimated signal if they enhance the correlation between the new estimate and the original signal, as anticipated by the ratio  $R_p$ . If not, the addition process is stopped, and the count number  $m$  remains fixed as  $\mathcal{M}_j$ . The core of the RTFT method consists of two matrices, where each column corresponds to a specific time interval, and the number of rows is determined by the selected order. The first matrix, referred to as Matrix  $\mathcal{F}$ , contains the frequencies ranked highest for each short-time segment. The second matrix, known as Matrix  $\mathcal{C}$ , includes the corresponding correlation

coefficients. Finally, it is worth mentioning that the parameters utilized in the windowing technique, such as window type, length, and amount of overlap, can influence the resulting spectrum and should therefore be selected carefully.

### 3. Experimental Results

In this section, the application of the proposed method specializes in analysing the most effective parts of an experimental multicomponent nonstationary signal. As depicted in Fig.2, a real-life experimental signal from vibration-based tool condition monitoring, consisting of a nonstationary multicomponent signal lasting 20 seconds in a 200-minute timeframe, was chosen to compare the proposed technique with other methods. The provided signal includes  $2 \times 10^5$  data points obtained at one-second intervals within each 10-minute data segment with a sampling rate of 10 kHz.

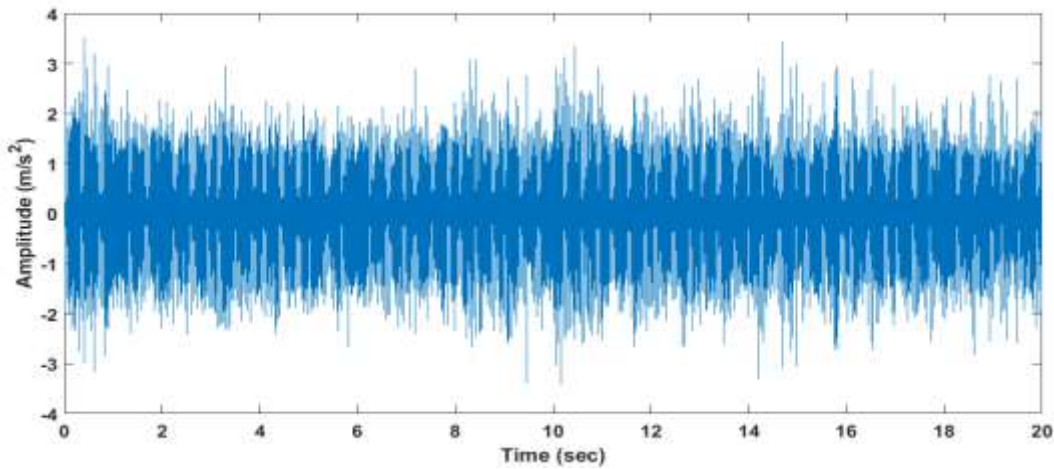
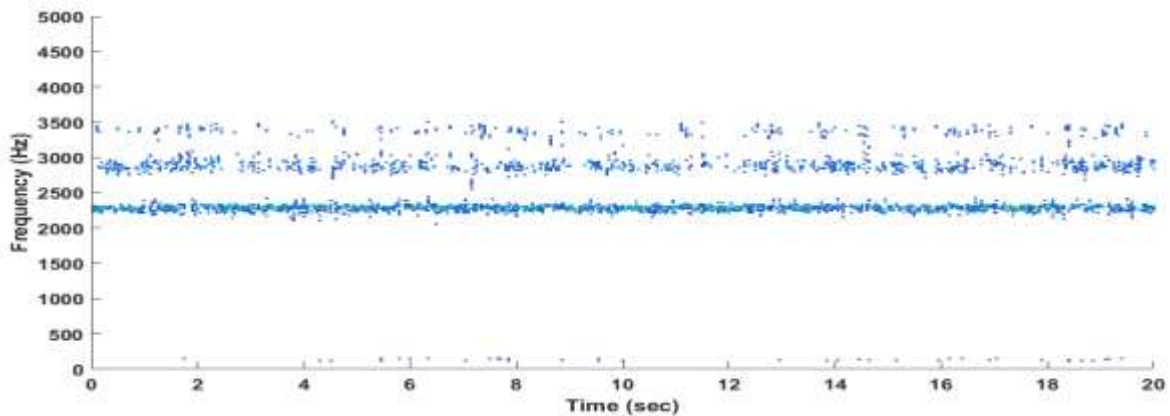
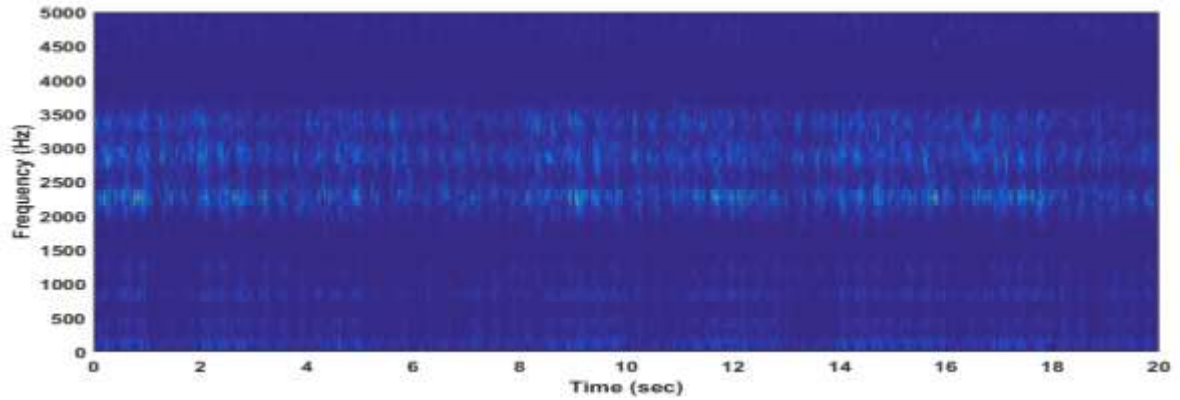


**Figure 2.** Experimental validation: TCM non-stationary signal

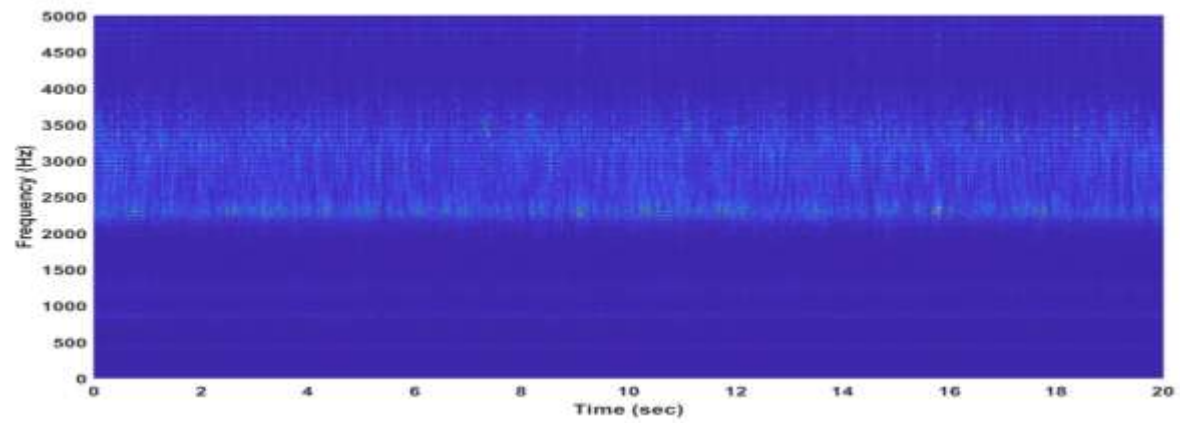
Fig. 3 illustrates the results of the implemented methods (3b-e) against the proposed method (3a) regarding this experimental signal. As discussed in previous numerical case study, the implementation of the HHT method was challenging, as shown in Fig 3.e.



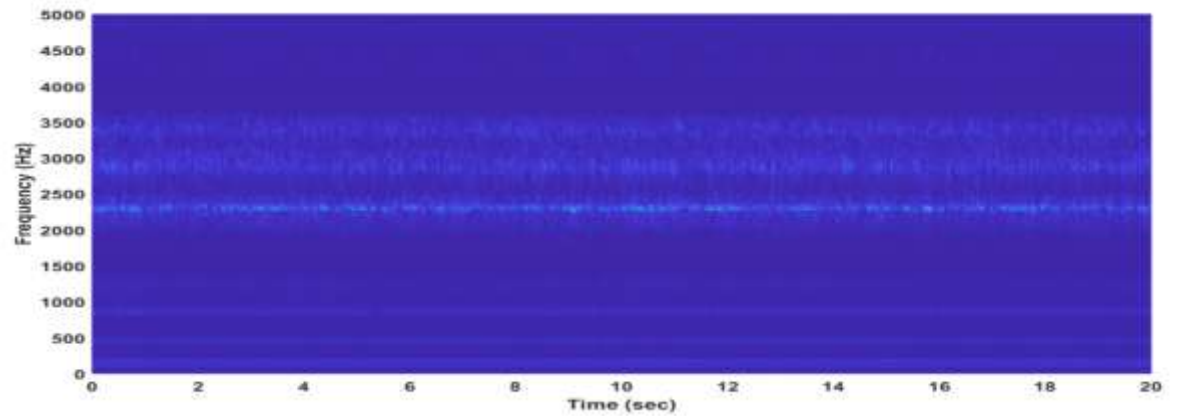
(a). The proposed Reduced-order Time-Frequency Transform (RTFT) technique



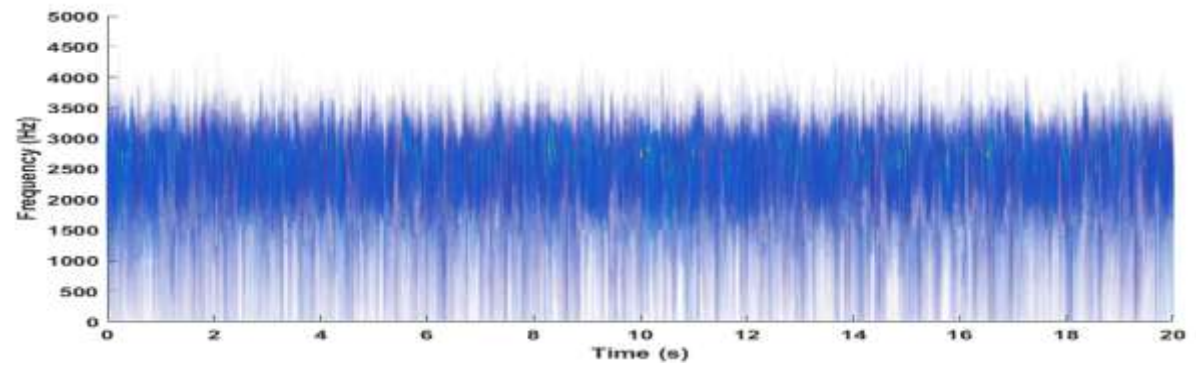
(b). The Short-Time Fourier Transform (STFT) Technique



(c). The Wavelet Synchrosqueezed Transform (WSST) technique



(d). The Fourier Synchrosqueezed Transform (FSST) technique



(e). The Hilbert-Huang Transform (HHT) technique

**Figure 3.** Joint time-frequency domain results

Considering the results within Fig. 3, it is observed that the most effective frequencies vary across different separated bands ranging from 2000 Hz to 3500 Hz, while other frequencies are not as relevant to the tool wear symptoms. Thus, it appears that the RTFT methodology yields a more distinct joint time-frequency spectra. Hence, having greater clarity compared to others can be seen as a significant advantage of the proposed method. To gain a better understanding of how the analysis of these spectrums results in the diagnosis of symptom failures, it is recommended to refer to the original paper which focuses on symptom recognition [24,25]. It is noteworthy that the following table provide a comparison based on the full data size. However, should there be a need to reduce the data volume, it is possible to imply the sparse theory in conjunction with these well-established methods. This approach facilitates a decrease in data size by prioritizing the largest volume, rather than considering the entirety of the dataset. Nevertheless, it is important to highlight that, similar to the original methodologies, the forthcoming tables incorporate a comparison of the full data size.

**Table 1.** The data size of the time-frequency Spectrum

STFT	128 × 6247
HHT	101 × 200000
WSST	416 × 200000
FSST	129 × 200000
RTFT*	28 × 400

As expected, the proposed technique, formulated as a reduced-order technique, leads to a smaller data volume in terms of the output matrix size. When considering the data volume of the results, it is important to emphasize the effect of the ratio of participation,  $R_p$ , in controlling the amount of transformed data.

## 4. Conclusion

Although time-frequency transform methods have been studied and implemented in a wide variety of research areas for decades, achieving more accurate results with less data volume remains an open problem. In light of this need, this research proposed a novel approach named the Reduced-Order Time-Frequency Transform (RTFT) technique, aimed at reducing the data volume in joint time-frequency domain results while not compromising accuracy or efficiency. The effectiveness of the suggested RTFT has been validated by comparing it with other well-established techniques. The vibration-based tool condition monitoring signal is analysed to demonstrate the superiority of the RTFT in reducing data volume while maintaining accuracy.

## REFERENCES

1. Kizilkaya, A., and Elbi, M. D., "A Fast Approach of Implementing the Fourier Decomposition Method for Non-linear and Non-Stationary Time Series Analysis," *Signal Processing*, Vol. 206, 2023, p. 108916. <https://doi.org/10.1016/j.sigpro.2022.108916>
2. Akan, A., and Cura, O. K., "Time-Frequency Signal Processing: Today and Future," *Digital Signal Processing*, Vol. 119, 2021, p. 103216. <https://doi.org/10.1016/j.dsp.2021.103216>
3. Lu, L., Ren, W.-X., and Wang, S.-D., "Fractional Fourier Transform: Time-Frequency Representation and Structural Instantaneous Frequency Identification," *Mechanical Systems and Signal Processing*, Vol. 178, 2022, p. 109305. <https://doi.org/10.1016/j.ymssp.2022.109305>
4. Cohen, L., "Time-Frequency Analysis, 778 Prentice Hall PTR," Englewood Cliffs, NJ, 1995.
5. Salles, R., Belloze, K., Porto, F., Gonzalez, P. H., and Ogasawara, E., "Nonstationary Time Series Transformation Methods: An Experimental Review," *Knowledge-Based Systems*, Vol. 164, 2019, pp. 274–291. <https://doi.org/10.1016/j.knosys.2018.10.041>
6. Yuan, P.-P., Zhang, J., Feng, J.-Q., Wang, H.-H., Ren, W.-X., and Wang, C., "An Improved Time-Frequency

- Analysis Method for Structural Instantaneous Frequency Identification Based on Generalized S-Transform and Synchroextracting Transform,” *Engineering Structures*, Vol. 252, 2022, p. 113657. <https://doi.org/10.1016/j.engstruct.2021.113657>
7. Dong, H., Yu, G., Lin, T., and Li, Y., “An Energy-Concentrated Wavelet Transform for Time-Frequency Analysis of Transient Signal,” *Signal Processing*, Vol. 206, 2023, p. 108934. <https://doi.org/10.1016/j.sigpro.2023.108934>
  8. Li, W., Auger, F., Zhang, Z., and Zhu, X., “Newton Time-Extracting Wavelet Transform: An Effective Tool for Characterizing Frequency-Varying Signals with Weakly-Separated Components and Theoretical Analysis,” *Signal Processing*, Vol. 209, 2023, p. 109017. <https://doi.org/10.1016/j.sigpro.2023.109017>
  9. Daubechies, I., Lu, J., and Wu, H.-T., “Synchrosqueezed Wavelet Transforms: An Empirical Mode Decomposition-like Tool,” *Applied and computational harmonic analysis*, Vol. 30, No. 2, 2011, pp. 243–261. <https://doi.org/10.1016/j.acha.2010.08.002>
  10. Sandsten, M., “Time-Frequency Analysis of Time-Varying Signals and Non-Stationary Processes,” Lund University, 2016.
  11. de Souza, U. B., Escola, J. P. L., and da Cunha Brito, L., “A Survey on Hilbert-Huang Transform: Evolution, Challenges and Solutions,” *Digital Signal Processing*, Vol. 120, 2022, p. 103292. <https://doi.org/10.1016/j.dsp.2021.103292>
  12. Rilling, G., Flandrin, P., and Goncalves, P., “On Empirical Mode Decomposition and Its Algorithms,” In *IEEE-EURASIP workshop on nonlinear signal and image processing*, Vol. 3, 2003, pp. 8–11.
  13. Zhou, W., Feng, Z., Xu, Y., Wang, X., and Lv, H., “Empirical Fourier Decomposition: An Accurate Signal Decomposition Method for Nonlinear and Non-Stationary Time Series Analysis,” *Mechanical Systems and Signal Processing*, Vol. 163, 2022, p. 108155. <https://doi.org/10.1016/j.ymsp.2021.108155>
  14. Gu, J., and Peng, Y., “An Improved Complementary Ensemble Empirical Mode Decomposition Method and Its Application in Rolling Bearing Fault Diagnosis,” *Digital Signal Processing*, Vol. 113, 2021, p. 103050. <https://doi.org/10.1016/j.dsp.2021.103050>
  15. Dragomiretskiy, K., and Zosso, D., “Variational Mode Decomposition,” *IEEE transactions on signal processing*, Vol. 62, No. 3, 2013, pp. 531–544. <https://doi.org/10.1109/TSP.2013.2288675>
  16. Singh, P., Joshi, S. D., Patney, R. K., and Saha, K., “The Fourier Decomposition Method for Nonlinear and Non-Stationary Time Series Analysis,” *Proceedings of the Royal Society A: Mathematical, Physical and Engineering Sciences*, Vol. 473, No. 2199, 2017, p. 20160871. <https://doi.org/10.1098/rspa.2016.0871>
  17. Brunton, S. L., and Kutz, J. N., “Data-Driven Science and Engineering: Machine Learning, Dynamical Systems, and Control,” Cambridge University Press, 2019.
  18. Auger, F., Flandrin, P., Lin, Y.-T., McLaughlin, S., Meignen, S., Oberlin, T., and Wu, H.-T., “Time-Frequency Reassignment and Synchrosqueezing: An Overview,” *IEEE Signal Processing Magazine*, Vol. 30, No. 6, 2013, pp. 32–41. <https://doi.org/10.1109/MSP.2013.2265316>
  19. Oberlin, T., Meignen, S., and Perrier, V., “The Fourier-Based Synchrosqueezing Transform,” presented at the 2014 IEEE international conference on acoustics, speech and signal processing (ICASSP), 2014.
  20. Qin, L., Yang, G., and Sun, Q., “Maximum Correlation Pearson Correlation Coefficient Deconvolution and Its Application in Fault Diagnosis of Rolling Bearings,” *Measurement*, Vol. 205, 2022, p. 112162. <https://doi.org/10.1016/j.measurement.2022.112162>
  21. Randall, R. B., and Antoni, J., “Why EMD and Similar Decompositions Are of Little Benefit for Bearing Diagnostics,” *Mechanical Systems and Signal Processing*, Vol. 192, 2023, p. 110207. <https://doi.org/10.1016/j.ymsp.2023.110207>
  22. Verma, A., Goyal, A., Kumara, S., and Kurfess, T., “Edge-Cloud Computing Performance Benchmarking for IoT Based Machinery Vibration Monitoring,” *Manufacturing Letters*, Vol. 27, 2021, pp. 39–41. <https://doi.org/10.1016/j.mfglet.2020.12.004>
  23. Das, R., and Inuwa, M. M., “A Review on Fog Computing: Issues, Characteristics, Challenges, and Potential Applications,” *Telematics and Informatics Reports*, 2023, p. 100049. <https://doi.org/10.1016/j.teler.2023.100049>
  24. Isavand, J., Kasaei, A., Peplow, A., Wang, X., and Yan, J., “A Reduced-Order Machine-Learning-Based Method for Fault Recognition in Tool Condition Monitoring,” *Measurement*, Vol. 224, 2024, p. 113906. <https://doi.org/10.1016/j.measurement.2023.113906>
  25. Isavand, J., Kasaei, A., Peplow, A., and Yan, J., “Enhancing Response Estimation and System Identification in Structural Health Monitoring through Data-Driven Approaches,” *Building Acoustics*, 2024, p. 1351010X231219662. <https://doi.org/10.1177/1351010X231219662>